Eur Radiol (2002) 12:2770–2775
DOI 10.1007/s00330-002-1306-5

G.A. Krombach
T. Schmitz-Rode
A. Prescher
E. DiMartino
J. Weidner
R.W. Günther

The petromastoid canal on computed tomography

Received: 6 March 2001
Revised: 22 November 2001
Accepted: 3 December 2001
Published online: 21 February 2002

G.A. Krombach (✉) · T. Schmitz-Rode
J. Weidner · R.W. Günther
Department of Diagnostic Radiology,
University of Technology,
Pauwelstrasse 30, 52057 Aachen,
Germany
e-mail: krombach@rad.rwth-aachen.de
Tel.: +49-241-8088332
Fax: +49-241-8888499

A. Prescher
Department of Anatomy,
University of Technology,
Pauwelstrasse 30, 52057 Aachen,
Germany

E. DiMartino
Department of Otorhinolaryngology,
University of Technology,
Pauwelstrasse 30, 52057 Aachen,
Germany

Abstract The objective was to assess visibility and anatomy of the petromastoid canal in high-resolution CT. Computed tomography images of 188 patients were reviewed for delineation of the petromastoid canal. This bony canal connects the mastoid antrum with the cranial cavity and houses the subarcuate artery and vein. The diameter, obtained in the middle portion of the canal, was compared with the diameter of the vestibular and cochlear aqueduct in all patients, and absolute values measured in 20 cases. Collimation was 1 mm in 164 and 2 mm in 24 examinations. Additionally, temporal bone of a cadaver was imaged and microdissected. The petromastoid canal was identified bilaterally in all 164 scans that were obtained with a slice thickness of 1 mm. In 5 of the 24 patients imaged with a collimation of 2 mm, the canal was not visible, most probably due to partial-volume effects. The petromastoid canal had the same diameter as the cochlear aqueduct in 42/44 (right/left), exceeded it in 66/61 and was smaller in 75/78 cases. In comparison to the vestibular aqueduct it had an equal diameter in 38/41 (right/left), exceeded it in 63/61, and was rated as smaller in 82/81 temporal bones. Diameters for the canals were: petromastoid canal 0.51±0.04 mm; cochlear aqueduct 0.57±0.03; and vestibular aqueduct 0.63±0.06 mm. Microdissection of the specimen revealed the entire course of the canal and demonstrated a similar appearance of the structure as in the images. The petromastoid canal can easily be identified on high-resolution, thin-slice CT images. Knowledge of the anatomy of this bony canal prevents misinterpretation as pathological structure, such as fracture line, which might occur if this structure is not known.

Keywords Temporal bone · Computed tomography · Petromastoid canal · Subarcuate artery

Introduction

Advances in the field of CT have revolutionized the evaluation of the middle and inner ear in the past two decades [1, 2]. High-resolution CT of the temporal bone has become the standard imaging technique for patients presenting with symptoms related to the labyrinth [3]. For interpretation of the images and accurate assessment of pathological changes, knowledge of the normal anatomical appearance of this complex region is crucial. Numerous studies addressing the small structures of the temporal bone have contributed to increased understanding of the radiological anatomy [4, 5, 6]; however, only a limited number of reports consider the petromastoid canal, which is also called subarcuate canaliculus [7, 8]. In radiology textbooks this bony canal is usually not mentioned and most often it is ignored in the routine interpretation of temporal bone scans.

The petromastoid canal connects the posterior fossa and the mastoid antrum and contains the subarcuate ar-

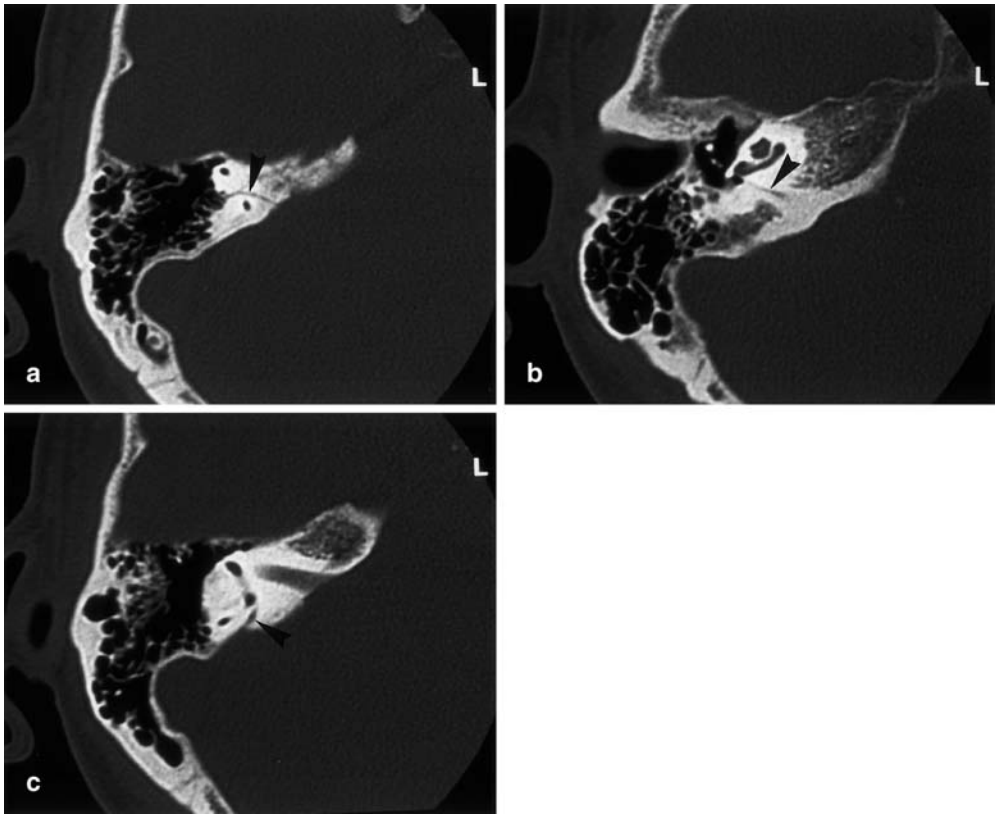

Fig. 1a–c Axial CT images of the temporal bone. **a** Petromastoid canal (*arrow*). The canal originates in the subarcuate fossa and passes with an anterior convex curve to the mastoidal cells. **b** Cochlear aqueduct. **c** Vestibular aqueduct. *Arrow* in **b** and **c** is position for comparison of the width of the aqueducts with the petromastoid canal

tery and vein. It arises from the subarcuate fossa, which is located superior to the internal auditory meatus at the posterior rim of the temporal bone, and passes between the two branches of the superior semicircular canal. It curves slightly anterior before it opens into the periantral mastoidal cells. The dura mater extends into the petromastoid canal; therefore, the canal can become a pathway for transmission of infections from the mastoid to the intracranial cavity and is a possible location for cerebrospinal fluid fistulas [8, 9]. Injury of the subarcuate artery during surgery can cause severe bleeding. To our knowledge, the CT features of the petromastoid canal have only been evaluated in small series of cadavers [8]. In recent reports it is still claimed as an inconstant structure [7, 8]. The purpose of this study was to address the frequency and appearance of the petromastoid canal on routine temporal bone CT scans in a series of 188 patients.

Additionally, the temporal bone of a cadaver was imaged with the same parameter protocol as used for evaluation of the patients and microdissected thereafter, in order to correlate the imaging characteristics with the anatomical appearance.

Materials and methods

Computed tomography images of normal temporal bones of 188 patients were reviewed to assess the presence and the size of the petromastoid canal. For this purpose, scans that were diagnosed as being normal were selected from the archived reports of 1999–2000. Ninety-eight female and 90 male patients (mean age 43 years, age range 9 months to 93 years) comprised our study population. In all patients both sides were investigated, resulting in altogether 376 evaluated temporal bones.

All images were obtained on a Tomoscan AV 1 scanner (Philips, Best, The Netherlands) in the sequential mode. The patients were imaged in the supine position and the gantry was tilted until a scan plane parallel to the orbitomeatal line was achieved. In order to reduce the radiation exposure of the patients' lenses, the head of the patient was reclined and the most superior slice positioned infraorbitally. Thereby, direct exposure of the lenses to primary radiation was avoided. In 164 patients slice thickness was 1 mm, carried out at a 1-mm interval. In the remaining 24 patients collimation was 2 mm. Scan parameters included a 512×512 matrix, 125 mA, 120 kV, and 4-s rotation time. A sharp (bone) filter with edge enhancement was applied. The field of view was adapted to the patients' size and included both temporal bones.

All images were photographed using a window width of 1600 HU, centered at 400 HU.

The scans were reviewed in consensus by two experienced radiologists. Both temporal bones were evaluated in all patients. First, the presence of the petromastoid canal was assessed. In the next step, the diameter of the middle portion of the petromastoid canal was compared with the size of the middle portion of the vestibular aqueduct and the cochlear aqueduct and scored as equal, smaller, or wider (Fig. 1). These semiquantitative measurements

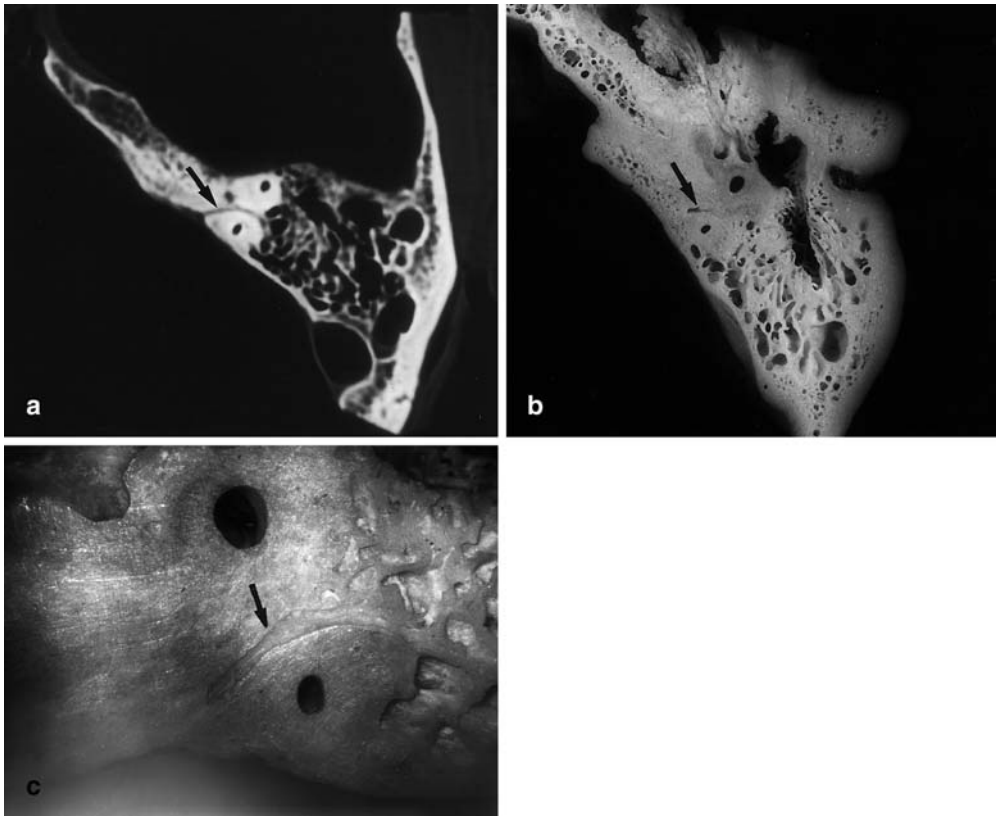

Fig. 2 **a** Axial CT image of left temporal bone of the cadaver of a 74-year-old man. The petromastoidal canal (*arrow*) passes through the arch of the anterior semicircular canal, slightly shifting to the posterior branch. **b** Horizontal section through the left temporal bone of the cadaver. **c** Detail from **b**. The canal opens to the retrocochlear cells

were obtained with a divider and carried out by the same radiologist. For statistical analysis the Kruskal-Wallis test was applied and age dependence of the presence and width of the subarcuate canal was assessed.

In 20 patients (10 men, 10 women; mean age 42 years) diameters of the petromastid canal, cochlear aqueduct, and vestibular acqueduct were measured on a workstation (EasyVision, Philips, Best, The Netherlands). For this purpose the digitally stored data were reloaded from magnetooptical disks to the CT scanner and transferred to the workstation via an internal network, with a DICOM protocol. Measurements were than carried out interactively, by placing a cursor over the middle portion of the canals.

In a cadaver, both temporal bones were scanned in the same orientation as in the patients, applying similar scanning parameters. The left temporal bone was macerated and dissected.

Results

The petromastoid canal was detected in 183 of the 188 cases on both sides.

The canal was visible in its whole course: It arises from the subarcuate fossa at the posterior rim of the temporal bone. The orifice is located at the level of the posterior branch of the superior semicircular canal, or between the two branches of the superior semicircular canal. The petromastoid canal travels between the two branches of the superior semicircular canal, slightly deviated to the posterior, nonampullary crus. As shown in Fig. 1, the shape of the entire canal is usually convex to the anterior. This appearance can vary, such that the canal shows a straighter course in some cases. After forming an anterior convex curve the canal opens into the periantral mastoidal cells (Fig. 1a). The orifice in the mastoidal cells is usually located more anterior than the orifice of the canal in the subarcuate fossa; however, this can vary, especially in cases in which the canal bends anterior more strongly. The mastoidal orifice of the petromastoid canal is located more posterior than the orifice in the subarcuate fossa.

Usually the petromastoid canal is completely surrounded by compact bone. As a variant in patients with strong pneumatization of the temporal bone the canal appears with a thin surrounding of compact bone, travelling between mastoidal cells. In such cases it can also be shorter, since it reaches the extended mastoidal cells after a shorter passage through the temporal bone.

In the scans, obtained with a collimation of 1 mm, the canal was visible in all cases. In 5 of the 24 patients, who were investigated with a slice thickness of 2 mm, the canals could not be delineated bilaterally.

In the cadaver CT showed the same orientation, course, and extension as in the patients. Microdissection revealed the entire course of the canal. The appearance of the canal resembled the imaging features (Fig. 2).

Table 1 Size of the petromastoid canal in comparison with the cochlear aqueduct and the vestibular aqueduct

	Petromastoid canal (%)					
	Equal		Larger		Smaller	
	Right	Left	Right	Left	Right	Left
Vestibular aqueduct	63, 34	61, 32.9	38, 20.8	41, 22.5	82, 45	81, 44.4
Cochlear aqueduct	66, 35.7	61, 32.9	42, 23	44, 24.1	75, 41.2	78, 42.8

Table 2 Size of the petromastoid canal, the cochlear aqueduct, and the vestibular aqueduct, measured in 20 patients (10 men, 10 women, mean age 42 years). *SEM* standard error of the mean; *SD* standard deviation. The first number in each field represents the absolute number, while the second number gives %

	Mean±SEM (mm)	SD (mm)
Petromastoid canal	0.51±0.04	0.21
Cochlear aqueduct	0.57±0.03	0.13
Vestibular aqueduct	0.63±0.06	0.25

Scoring of the diameter of the petromastoid canal in comparison with the cochlear aqueduct and the vestibular aqueduct was possible in all 183 patients in whom the canal was visible on both sides. On the right side, the diameter of the petromastoid canal was scored as equal to the cochlear aqueduct in 42 patients (23%), larger in 66 cases (35.7%), and smaller in 75 cases (41.2%). On the left side it was equal to the cochlear aqueduct in 44 cases (24.1%), larger in 61 patients (32.9%), and smaller in 78 cases (42.8%). In most of the patients the petromastoid canal was smaller than the cochlear aqueduct ($p<0.001$).

In comparison with the vestibular aqueduct the diameter of the petromastoid canal was scored as equal in 38 patients (20.8%), smaller in 82 cases (45%), and larger in 63 cases (34%) on the right side. On the left side the diameter was rated as equal to the diameter of the vestibular aqueduct in 41 cases (22.5%), smaller in 81 cases (44.4%), and larger in 61 cases (32.9%). Again, the petromastoid canal was smaller as the vestibular aqueduct in most of the patients ($p<0.001$). These results are summarized in Table 1. Rating of the size of the petromastoid canal in comparison with the cochlear aqueduct and the vestibular aqueduct correlated significantly for both sides ($p<0.001$). There was no statistically significant age dependence of the width of the petromastoid canal ($p=0.933$). Values for direct measurements of the canal are shown in Table 2.

The canal develops from the subarcuate fossa, which stretches out and narrows in the first 4 years. Two patients of our study population were younger than 4 years. In both of these patients the petromastoid canal was wide, according to this development (Fig. 3).

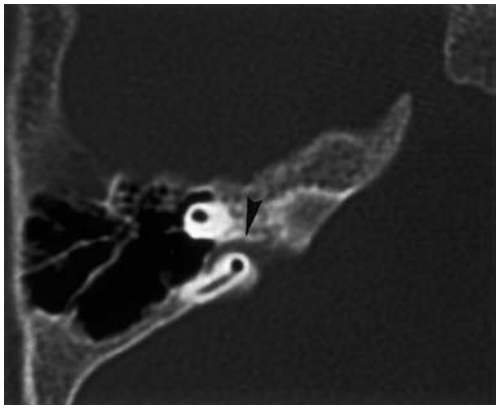

Fig. 3 A 9-month-old child. Axial CT image. The petromastoidal canal is still wide (*arrow*). It attains its canaliculous shape within the first 4 years

Discussion

The petromastoid canal was first described in 1904 by Mouret and Rouviere as an inconstant structure, which straightly travels from the mastoid antrum to the intracranial fossa [9]. With improving preparation techniques the canal was more frequently found in the temporal bone of adults [7, 10]; however, even in a recent report it is referred to as an inconstant structure that develops from the subarcuate fossa and "can persist in the adult" [8]. With introduction of high-resolution CT of the temporal bone into the clinical routine an extensive database of anatomical information has become available for assessment of the frequency and appearance of this canal. We could identify the petromastoidal canal in all temporal bones of our series, which were imaged with a slice thickness of 1 mm.

The petromastoidal canal arises from the subarcuate fossa, which is located at the posterior rim of the temporal bone, courses between the two limbs of the superior semicircular canal, and opens into the periantral mastoidal cells. It is slightly shifted to the posterior, nonampullary crus of the anterior semicircular canal and forms an anterior convex curve. The canal is lined by dura mater and contains the subarcuate artery and vein. The subarcuate artery mostly originates directly from the anterior

inferior cerebellar artery or less frequently from the basilar artery or from the internal auditory artery. It supplies the otic capsule in the area of the semicircular canals, the posteriosuperior wall of the vestibule, and the medial wall of the antrum mastoideum [10]. The artery usually has anastomoses to dural branches of the posterior meningeal artery and to branches of the external carotid artery in the middle ear and to branches of the stylomastoid artery [11]. During surgery for removal of acusticus neurinomas inadvertent injury of the subarcuate artery can result in troublesome bleeding; however, due to the well-pronounced anastomoses, coagulation of this vessel is well tolerated.

The petromastoidal canal develops from the subarcuate fossa, which is a huge cavity in the fetus. It reaches from the posterior fossa to the region, which subsequently develops to the mastoid. In the first 5 years, the fossa subarcuata narrows and attains a canaliculous shape [12]. In primates, it persists and houses the petrosal lobule of the cerebellar paraflocculus [13]. The onto- and phylogenetic development explains that the petromastoid canal remains dura-lined in the adult human. This feature makes it prone to development of congenital or acquired cerebrospinal fluid fistulas [14]. In surgical interventions, elevation of the dura along the posterior fossa surface of the temporal bone can result in a dural tear at the orifice of the petromastoidal canal, which can cause a cerebrospinal fluid leak [8]; however, the orifice of the canal can serve as an anatomical landmark during surgery. Assessment of the position of the subarcuate canal in relation to the other landmarks prior to surgery can be helpful for orientation during the intervention as well as in order to prevent inadvertent injury of the subarcuate artery.

Furthermore, the petromastoid canal gains clinical importance as a pathway for transmission of infections spreading from the mastoidal cells to the dura and the intracranial cavity.

For interpretation of CT images of the temporal bone in traumatized patients knowledge of the course of the subarcuate canal is important, as this structure could be mistaken as a fracture line.

The canal was invariably visible in scans obtained with a collimation of 1 mm in our series. Scoring of the diameter of the petromastoid canal demonstrated it as having the same size as the vestibular aqueduct or being smaller in 83% of our cases. Direct measurement revealed a diameter of less than 1 mm for the petromastoid canal (0.51±0.04 mm). The vestibular aqueduct has been reported to measure approximately 1 mm in cadavers [15], whereas we obtained a diameter of 0.63±0.06 from CT scans. These results correspond to previous reports, where the width of the petromastoid canal was found to be approximately 1 mm in cadavers [7, 8].

Partial-volume effects can render the detection of structures, which are half the size of the slice thickness, impossible. This is the most probable cause for lacking delineation of the petromastoidal canal in 5 patients in this series. In these cases the images were obtained with a slice thickness of 2 mm, which is double the diameter of the canal. Correspondingly, the cochlear and vestibular aqueduct were also not visible. This strongly supports the argument of partial-volume effects, as these canals are known to be invariable structures. The petromastoidal canal was delineated in all patients when imaged with a slice thickness of 1 mm. Therefore, the petromastoid canal has to be considered as a structure that is regularly visible within the temporal bone on high-resolution CT.

Comparison of the width of the petromastoid canal and the vestibular and cochlear aqueduct showed no age dependence. In our study population, only 2 patients were younger than 4 years. In both of these cases, the petromastoid canal was still wide; however, no statistical significance could be found, according to the small number of young children in this series. These results support that the petromastoid canal remains unchanged in the adult after it achieves its diameter in the young child [12].

In conclusion, the petromastoid canal is easily identified in its entire course on axial high-resolution CT images with a slice thickness of 1 mm, obtained at the level of the superior semicircular canal. Knowledge of the anatomy of this structure prevents misinterpretation and can facilitate diagnosis, as this structure has clinical importance for development of cerebrospinal fluid fistulas and transmission of infections. Furthermore, it serves as an anatomical landmark for surgical interventions.

Acknowledgement The authors thank R. Minkenberg, Institute for Biometry, University of Technology, Aachen, Germany, for statistical analysis.

References

1. Swartz DJ (1989) Current imaging approach to the temporal bone. Radiology 171:309–317
2. Lustrin ES, Robertson RL, Tilak S (1994) Normal anatomy of the skull base. Neuroimaging Clin North Am 4:465–478
3. Hermans R, Marchal G, Feenstra L, Baert AL (1995) Spiral CT of the temporal bone: value of image reconstructions at submillimetric table increments. Neuroradiology 37:150–154
4. Fatterpekar GM, Mukherji SK, Lin Y, Alley JG, Stone JA, Castillo M (1999) Normal canals at the fundus of the internal auditory canal: CT evaluation. J Comput Assist Tomogr 23:776–780
5. Swartz JD (1990) The temporal bone: imaging considerations. Crit Rev Diagn Imaging 30:341–417
6. Alexander AE Jr, Caldemeyer KS, Rigby P (1998) Clinical and surgical application of reformated high-resolution CT of the temporal bone. Neuroimaging Clin North Am 8:631–650

7. Proctor B (1983) The petromastoid canal. Ann Otol Rhinol Laryngol 92:640–644
8. Tekdemir I, Aslan A, Elhan A (1999) The subarcuate canaliculus and its artery: a radioanatomical study. Ann Anat 181:207–211
9. Mouret J, Rouviere H (1904) The petromastoid canal. L' Assoc des Anatomistes 6th session, Toulouse, France
10. Wilbrand H, Rauschning W, Ruhn G (1986) The subarcuate fossa and channel. A radioanatomic investigation. Acta Radiol Diagn 27:637–644
11. Kim HN, Kim YH, Park IY, Kim RG, Chung IH (1990) Variability of the surgical anatomy of the neurovascular complex of the cerebellopontine angle. Ann Otol Rhinol Laryngol 99:288–296
12. Hilding DA (1987) Petrous apex and subarcuate fossa maturation. Laryngoscope 97:1129–1135
13. Gannon PJ, Eden AR, Laitman JT (1988) The subarcuate fossa and cerebellum of extant primates: comparative study of a skull-brain interface. Am J Phys Anthropol 77:143–164
14. Gacek RR, Leipzig B (1979) Congenital cerebrospinal otorrhea. Ann Otol Rhinol Laryngol 88:358–365
15. Lang J, Hack C (1985) Position and variations in the position of the canal system in the temporal bone. I. The canals of the pars petrosa between the margo superior and the meatus acusticus internus. HNO 33:176–179